

## Article

# Investigation on the Dynamic Characteristics of a New High-Pressure Water Hydraulic Flow Control Valve

Wenchao Liu <sup>1,2</sup>, Jie Tian <sup>1,2,\*</sup>, Hongyao Wang <sup>1,2</sup>, Junshi Li <sup>3</sup>, Rulin Zhou <sup>3</sup> and Yu Cao <sup>1</sup>

<sup>1</sup> School of Mechanical and Electrical Engineering, China University of Mining & Technology-Beijing, Beijing 100083, China; liuwc56@foxmail.com (W.L.); 201501@cumtb.edu.cn (H.W.); bqf2100406029@cumtb.edu.cn (Y.C.)

<sup>2</sup> Key Laboratory of Intelligent Mining and Robotics, Ministry of Emergency Management, Beijing 100083, China

<sup>3</sup> Beijing Tianma Intelligent Control Technology Co., Ltd., Beijing 101399, China; lij@s@tdmarco.com (J.L.); zhoul@tdmarco.com (R.Z.)

\* Correspondence: tianj@cumtb.edu.cn

**Abstract:** Water has the disadvantages of low viscosity, poor lubrication, and easy leakage, which leads to many problems in water hydraulic flow control valves, such as low working pressure and large flow fluctuations. To address these issues, this paper proposes a novel digital flow control valve. The valve uses a linear stepper motor as the driving device. Compared to proportional electromagnets, the thrust and stroke of the linear stepper motor are larger, making the valve more suitable for high-pressure working conditions. Simultaneously, the valve innovatively incorporates a set of pilot valve spool strings at the front end of the pilot valve damping hole. Through controlling the two pilot valves to regulate the pressure difference before and after the damping hole, the flow passing through the pilot valve is maintained stable, thereby making the pressure of the upper chamber of the master valve spool more stable. In comparison to a single pilot valve structure, this design ensures a more stable main valve core position and reduces flow fluctuation. A mathematical and simulation model of the valve has been established, confirming the performance advantages of the new structure. The impact of structural parameters (such as valve core diameter, spring stiffness, and diameter of damping hole) on the stability of flow regulation has been investigated. A genetic algorithm has been employed to optimize the key parameters that influence valve flow stability, resulting in the identification of optimal parameters. The simulation results indicate that the optimized parameters lead to a reduction of approximately 45% in the maximum overshoot oscillation amplitude of the valve flow regulation. A prototype of the new flow control valve was developed, and a test system was established for conducting tests. The test results also confirmed the performance advantages of the valve and the accuracy of the optimal design.

**Keywords:** water hydraulic system; flow control; digital flow control valve; genetic algorithm; optimization



**Citation:** Liu, W.; Tian, J.; Wang, H.; Li, J.; Zhou, R.; Cao, Y. Investigation on the Dynamic Characteristics of a New High-Pressure Water Hydraulic Flow Control Valve. *Machines* **2024**, *12*, 640. <https://doi.org/10.3390/machines12090640>

Academic Editor: Davide Astolfi

Received: 28 July 2024

Revised: 4 September 2024

Accepted: 9 September 2024

Published: 12 September 2024



**Copyright:** © 2024 by the authors. Licensee MDPI, Basel, Switzerland. This article is an open access article distributed under the terms and conditions of the Creative Commons Attribution (CC BY) license (<https://creativecommons.org/licenses/by/4.0/>).

## 1. Introduction

Water hydraulic technology is a crucial area of development with a wide range of applications in marine exploration, coal mining, and other fields [1–3]. However, hydraulic components used in water media are susceptible to issues such as leakage, inadequate lubrication, and cavitation [4,5]. Therefore, the development of water hydraulic components based on the characteristics of water hydraulic systems holds significant importance.

Flow control plays a crucial role in hydraulic systems, and the speed regulating valve is a commonly used type of valve for flow control. Typically, a speed regulating valve consists of a series arrangement of a differential pressure reducing valve and a throttle valve. As the load pressure changes, the opening of the differential pressure reducing valve adjusts accordingly to maintain the pressure difference before and after the throttle

valve constant. This ensures that the flow controlled by the speed regulating valve remains stable and unaffected by load changes [6,7]. However, the speed regulating valve has poor anti-interference ability, leading to significant flow overshoot when the load changes. Additionally, it suffers from drawbacks such as slow response speed and poor adjustment accuracy [8,9]. These limitations are particularly pronounced in water hydraulic systems, making the speed control valve unsuitable for such applications.

The throttle valve is also a common flow control valve in hydraulic systems, and it can be categorized into two types based on the driving mode: direct drive type and pilot stage control type [10]. The direct drive throttle valve adjusts the opening of the valve core directly through the proportional electromagnet and other driving devices, which has the characteristics of high control precision and fast response speed [11,12]. However, the limited thrust and stroke of the proportional solenoid make it difficult to apply this structure under high-pressure conditions. As a result, many scholars have proposed a two-stage proportional valve structure with pilot stage control in order to address this issue.

Anderson initially proposed a two-stage flow control valve with displacement and hydraulic feedback. The pilot stage of the valve is directly proportional to the main stage flow, and the main stage flow can be adjusted by manipulating the pilot stage flow. Despite its wide range of applications, this valve also has some drawbacks. For instance, it exhibits low flow regulation accuracy when the load undergoes significant changes [13]. In order to address this issue, scholars have conducted research. Han et al. proposed the use of displacement sensors to directly detect the displacement of the main valve core and control the valve core opening through feedback algorithms in order to enhance the accuracy of main valve core position control. However, this approach complicates the structural design of the valve and necessitates higher pressure resistance characteristics and stability of the displacement sensor [14]. Other scholars have proposed precise flow control methods based on various compensators. For example, Erikson proposed a mechanical pressure compensation controller, Huang proposed a digital pressure compensation controller, and Tian proposed an artificial neural network compensation controller [15].

However, the majority of the aforementioned research focuses on oil hydraulic systems. The proportional throttle valves utilized in these studies all feature a slide valve structure in their pilot stage. Due to the low viscosity of water and its propensity for easy leakage, they may exhibit internal leakage under high-pressure conditions, thereby impacting flow regulation effectiveness and stability. In order to achieve flow control in water hydraulic systems, scholars have conducted research on developing a water medium proportional speed control valve based on the structure of the oil medium proportional speed control valve. Park has optimized the gap between the main valve core and valve sleeve, and added a pressure equalization groove in the main valve core to prevent hydraulic locking. Subsequently, experiments were conducted to verify the feasibility of the developed water-based proportional speed control valve. However, the maximum flow rate of the valve is only 14 L/min, which is not suitable for hydraulic systems with high flow rates [16]. Park also proposed a water flow control valve that utilizes a high-speed on/off valve as the pilot stage. The valve employs the leakage flow between the main valve core and valve sleeve as the pilot liquid flow, and can achieve flow control by adjusting the pulse frequency. However, the maximum pressure of the valve is 14 MPa, which makes it unsuitable for high-pressure working conditions [17].

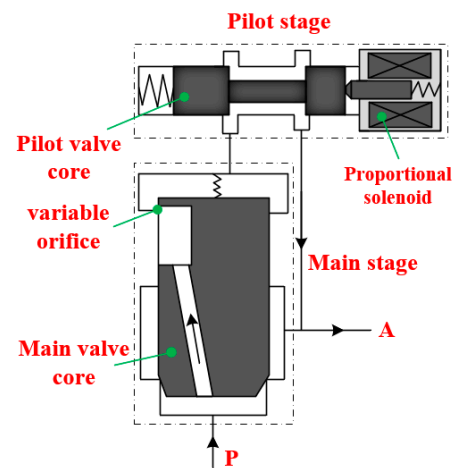
Based on the literature analysis above, it is evident that existing flow control valves may encounter issues such as leakage and poor flow stability when utilized in high-pressure water conditions. To address these challenges, this article presents a novel high-pressure water medium flow control valve that utilizes a two-stage valve core structure. This new design incorporates two pilot stages to enhance flow control stability and employs a slide valve structure to minimize leakage. The main stage employs a plug-in valve structure. The performance advantages have been confirmed through the establishment of mathematical models and simulation models. The key structural parameters of the digital flow control valve were optimized using a genetic algorithm, thereby improving the dynamic response

characteristics of the valve. The performance advantages and accuracy of the optimized valve design have been confirmed through experimental validation.

## 2. New Structure Digital Flow Control Valve

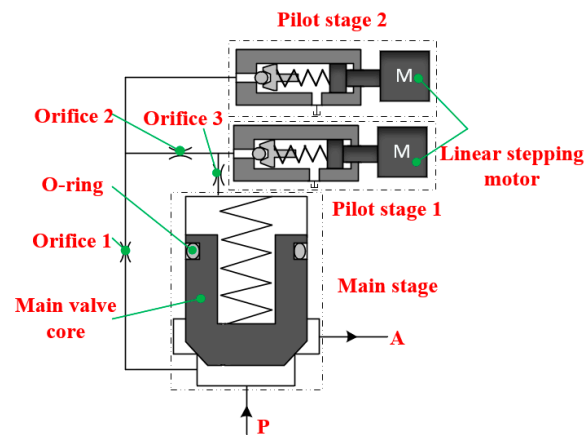
### 2.1. Structure and Principle of Valves

Figure 1 illustrates a typical proportional flow control valve in an oil hydraulic system, with its pilot stage adopting a slide valve structure. However, due to the low viscosity of water, there is a high likelihood of leakage at the pilot spool. Additionally, there exists a gap between the main spool and the valve sleeve, resulting in a pressure difference between the upper cavity of the main spool and working port A. This allows water medium to easily enter the gap, thereby affecting the stability of the main spool position. Furthermore, a variable damping hole is formed between the main spool and valve sleeve. As a result of this unstable position of the main spool, both pressure and flow rate of water medium through the variable damping hole are prone to fluctuation. Consequently, it becomes challenging to apply this structure in high-pressure water hydraulic systems.



**Figure 1.** Typical structure of a proportional flow control valve.

Figure 2 depicts the structural diagram of the new high-pressure water hydraulic flow control valve proposed in this paper. The valve features a two-stage spool structure, with the main stage comprising a main spool. The main spool inlet P is connected to the high-pressure water, while outlet A is connected to the load. Additionally, the main spool is equipped with a sealing ring slot and installed with a sealing ring to prevent leakage between the main spool and the valve sleeve, thereby ensuring effective adjustment of the valve spool position. The pilot stage consists of two pilot valves and three damping holes. Damping hole 1's inlet is connected to the main spool inlet, and its outlet is connected to pilot valve 1's inlet and damping hole 2's inlet. Damping hole 2's outlet is linked to damping hole 3's inlet and pilot valve 2's inlet, while damping hole 3's outlet connects to the main spool upper cavity. Finally, both pilot valves' outlets are directly connected to the liquid tank. Considering the traditional slide valve structure's tendency to experience significant leakage under high-pressure water conditions, each pilot valve adopts a ball valve structure. Additionally, the pilot spring is directly compressed by the linear stepping motor in order to control the pressure value of the valve inlet.



**Figure 2.** Structure of a new high-pressure water hydraulic flow control valve.

The main working principle is as follows: In the initial state, high-pressure water from the pump enters the lower chamber of the main spool and then flows into the upper chamber of the main spool through damping holes 1, 2, and 3. At this point, with pilot valves 1 and 2 in a closed state, both chambers of the main spool have equal pressure, resulting in the main spool being in a closed state. With the opening of pilot valve 1, the pressure in the upper chamber of the main spool is reduced due to throttle pressure loss in damping holes 1 and 2. This leads to a disruption in the force balance of the main spool, causing it to move upward until a new force balance position is reached. The linear stepper motor adjusts the pilot valve 1, thereby changing the compression of the pilot spring. This adjustment can alter the pressure of the upper chamber of the main spool, subsequently leading to a change in the position of the main spool. Ultimately, this process achieves flow regulation as intended. Compared to a proportional electromagnet, a linear stepper motor offers greater thrust and stroke, making it better suited for high-pressure conditions. Additionally, its control accuracy is also higher. Because of the low viscosity of the emulsion, it will result in relatively large flow and pressure fluctuations as it passes through the damping hole and pilot valve. This leads to fluctuations in the pressure of the upper chamber of the main valve spool, which can easily cause oscillation of the main valve spool and affect the flow regulation effect. Pilot valve 2 has been incorporated into the structure to regulate the inlet pressure of damping hole 2 by controlling the linear stepping motor of pilot valve 2. This ensures that the pressure difference between the front and back of damping hole 2 remains constant, thereby maintaining a consistent flow rate through both damping hole 2 and pilot valve 1. As a result, this approach reduces pressure fluctuations in the upper chamber of the main valve core and enhances system flow stability.

## 2.2. Mathematical Model

The flow rate through the main spool can be expressed by the following formula:

$$q_1 = C_d \pi d_1 x_1 \sin \theta \sqrt{\frac{2(p_1 - p_3)}{\rho}} \quad (1)$$

where  $q_1$  is the flow through the main spool,  $C_d$  is the flow coefficient,  $d_1$  is the main spool seal diameter,  $x_1$  is the displacement of the main valve core,  $\theta$  is the half cone angle of the main valve core,  $p_1$  is the inlet pressure of the main valve core,  $p_3$  is the outlet pressure of the main valve core, and  $\rho$  is the density of water.

Upon analyzing Formula (1), it is evident that the flow rate through the main valve core is primarily influenced by the inlet pressure, outlet pressure, and displacement of the main valve core. The inlet pressure is controlled by the overflow valve at the pump outlet, while the outlet pressure is determined by the load. The displacement of the main valve

core can be analyzed by examining the force acting on it, which can be expressed using the following formula:

$$p_1 A_1 = p_2 A_2 + mg + k_1(x_1 + x_0) + F_a + F_f \quad (2)$$

where  $A_1$  is the effective area of the lower chamber of the main valve core,  $p_2$  is the pressure in the upper chamber of the main valve core,  $A_2$  is the effective area of the upper chamber of the main valve core,  $m$  is the quality of the main valve core,  $g$  is the gravitational acceleration,  $k_1$  is the stiffness of the main valve spring,  $x_0$  is the initial compression amount of the main valve spring,  $F_a$  is the steady-state hydraulic force of the main valve core, and  $F_f$  is the frictional force exerted on the main valve core.

Considering that factors such as friction, spring force, and hydraulic force are relatively small, the opening of the main valve core is primarily influenced by the pressure in the upper chamber of the main valve core. This pressure can be expressed by the following formula:

$$q_2 = C_d \pi d_2 x_2 \frac{\sqrt{\left(\frac{D}{2}\right)^2 - \left(\frac{d_2}{2}\right)^2}}{\frac{D}{2}} \sqrt{\frac{2p_2}{\rho}} \quad (3)$$

where  $q_2$  is the flow rate through pilot valve 1,  $d_2$  is the aperture of the pilot valve seat,  $x_2$  is the displacement of the pilot valve core, and  $D$  is the diameter of the ceramic ball of the pilot valve core.

The pressure in the upper chamber of the main valve core is primarily influenced by the flow rate through the pilot valve and the displacement of the pilot valve core. The flow rate through the pilot valve core is equivalent to the flow rate through damping hole 2, which can be represented by the following formula:

$$q_2 = C_d d_3 \sqrt{\frac{2(p_4 - p_2)}{\rho}} \quad (4)$$

where  $d_3$  is the diameter of damping hole 2 and  $p_4$  is the inlet pressure of damping hole 2.

In the structure of the flow control valve, the control algorithm can be utilized to adjust pilot valve 2 in order to maintain a constant pressure difference between the front and back of damping hole 2. This ensures that the flow rate through damping hole 2 and pilot valve 1 remains essentially unchanged, thereby enhancing the stability of pressure in the upper chamber of the main valve spool and subsequently improving the stability of flow through the main valve spool.

### 2.3. Simulation Model

To verify the flow regulation characteristics of the new structure flow control valve, a simulation model depicted in Figure 3 was constructed using AMESim2019.2 simulation software.

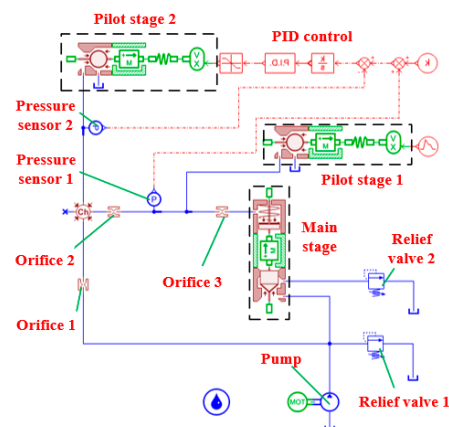


Figure 3. Simulation model.

In the simulation model, a relief valve is connected in series at the outlet of the main valve core to simulate the load. Additionally, a relief valve is connected in parallel at the inlet of the main valve core to regulate the flow control valve inlet pressure. Pressure sensors are installed at the inlets of pilot stage 1 and pilot stage 2, respectively, to adjust the spring compression of pilot stage 2 based on pressure feedback. This ensures that the pressure difference before and after damping hole 2 is always maintained at 10 bar. The simulation model was utilized to validate the flow regulation capability and stability of the flow control valve under high and low pressure conditions. The key technical parameters of the simulation model are presented in Table 1. The simulation duration was set to 11 s, and the simulation time interval was set to 0.01 s.

**Table 1.** Main technical parameters of simulation model.

Parameter Name	Value
Pilot valve seat diameter (mm)	5.5
Pilot valve spool diameter (mm)	20
Pilot valve spring stiffness (N/mm)	70
Diameter of damping hole 1 (mm)	1.2
Length of damping hole 1 (mm)	6
Diameter of damping hole 2 (mm)	1
Length of damping hole 2 (mm)	6
Diameter of damping hole 3 (mm)	0.8
Length of damping hole 3 (mm)	6
Main valve core sealing diameter (mm)	14
Main valve core diameter (mm)	16
relief valve 1 cracking pressure (bar)	200
relief valve 2 cracking pressure (bar)	120
Main spring stiffness (N/mm)	23.5
Main valve core quality (kg)	0.1
Half cone angle of main valve core (°)	30
Proportional gain of PID controller	1
Emulsion pump flow rate (L/min)	200

Under low-pressure conditions, the relief valve at the inlet of the main spool is set to open at 70 bar, while the relief valve at the outlet of the main spool is set to open at 15 bar. The spring compression of pilot stage 1 is depicted in Figure 4a. The extension of the motor shaft is 1.5 mm in 0–3 s, and it varies uniformly from 1.5 mm to 1.45 mm in 3–4 s. The extension of the motor shaft is 1.45 mm in 4–7 s, and it varies uniformly from 1.45 mm to 1.4 mm in 8–9 s. The extension of the motor shaft is 1.4 mm in 9–11 s. And the flow rate through the main spool throughout the process is documented in Figure 4b. Under high-pressure conditions, the opening pressure of the relief valve at the inlet of the main spool is set to 200 bar, and the opening pressure of the relief valve at the outlet of the main spool is set to 120 bar. The spring compression of pilot stage 1 is set as shown in Figure 4a. The extension of the motor shaft is 1.4 mm in 0–3 s, and it varies uniformly from 1.4 mm to 1.35 mm in 3–4 s. The extension of the motor shaft is 1.35 mm in 4–7 s, and it varies uniformly from 1.35 mm to 1.3 mm in 8–9 s. The extension of the motor shaft is 1.3 mm in 9–11 s. And the flow rate through the main spool during the whole process is recorded as shown in Figure 4b. The curve demonstrates that the flow can be adjusted by modifying the compression of the pilot spring. The flow curve remains stable under low pressure conditions, with a slight increase in flow fluctuation under high-pressure conditions. The proposed structure of the flow regulating valve is suitable for controlling flow under high-pressure water medium conditions, and it exhibits high stability in flow regulation.



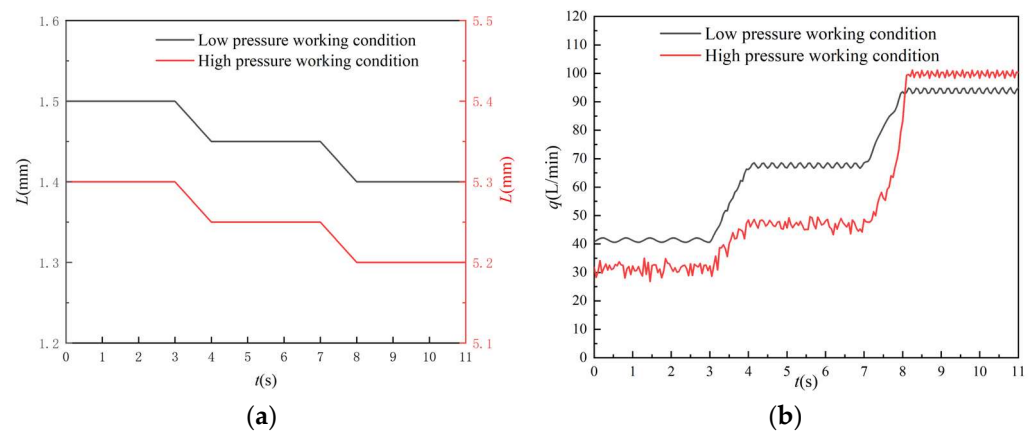


**Figure 4.** Simulation results. (a) Compression curve of pilot spring; (b) flow curve.

### 3. Optimization of Key Parameters for a New Digital Flow Control Valve Structure

#### 3.1. The Impact of Key Parameters on Flow Control Characteristics

Based on experience and the current literature, it has been found that valve parameters (such as valve core diameter, spring stiffness, and diameter of damping hole) have a significant impact on flow dynamic performance. Therefore, it is essential to conduct detailed research and optimize the key parameters of the valve through algorithms in order to improve its dynamic characteristics [14]. This paper presents the simulation model depicted in Figure 5, which is developed based on AMESim. The outlet of the flow control valve is connected to a pressure sensor, a flow sensor, and a proportional relief valve. The proportional relief valve is utilized to regulate the outlet pressure of the flow control valve, while the data from the pressure sensor and flow sensor are fed back to the controller. The inlet of the flow control valve is connected to a relief valve in order to maintain constant inlet pressure. Pressure sensors are respectively connected to the front and rear of damping hole 2, and their feedback is sent to the controller.

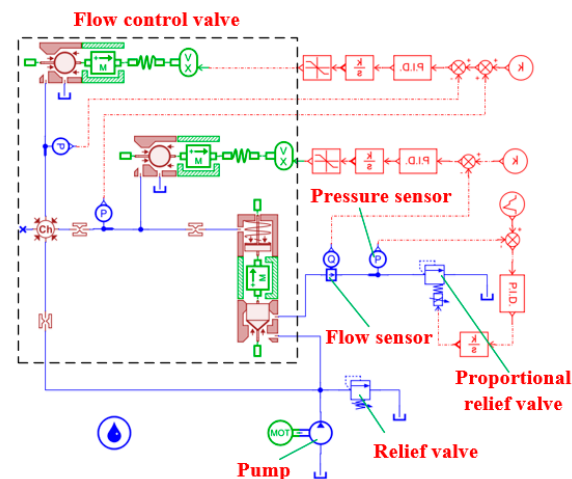


**Figure 5.** AMESim simulation model.

In this system, the flow target value through the main valve core is always set to 50 L/min, the outlet pressure target value of the flow control valve is always 40 bar, and the inlet pressure target value steps from 60 bar to 70 bar. The changes in the flow rate through the main valve core are monitored during the pressure change process. The main technical parameters of digital sequence valves and hydraulic systems are shown in Table 1. In this system, the target flow value through the main spool is consistently set at 60 L/min. The inlet pressure of the flow control valve is maintained at 70 bar, while the outlet pressure target value suddenly changes from 20 bar to 25 bar. It is important to monitor the change

in flow rate through the main spool under different parameters during sudden pressure changes. The primary technical parameters of the simulation model are presented in Table 1. The simulation duration was set to 5 s, and the simulation time interval was set to 0.01 s.

### 3.1.1. The Influence of the Diameter of Damping Hole 1 on Flow Rate Variation

Figure 6 illustrates the impact of the diameter of damping hole 1 on the flow through the main spool. The simulation results indicate that the diameter of damping hole 1 does not affect flow regulation. As the diameter of damping hole 1 increases, there is minimal change in both the amplitude and response time of flow regulation.

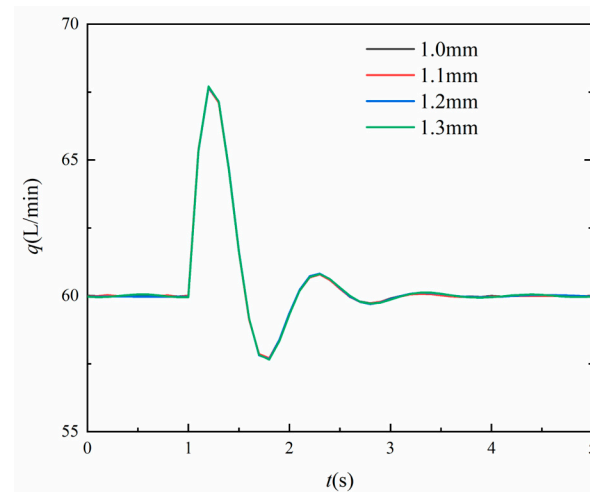


**Figure 6.** Flow curve under various diameters of damping hole 1.

### 3.1.2. The Influence of the Diameter of Damping Hole 2 on Flow Rate Variation

Figure 7 illustrates the impact of the diameter of damping hole 2 on the flow through the main spool. The simulation results indicate that the diameter of damping hole 2 has minimal influence on flow regulation. As the diameter of damping hole 2 increases, there is only a slight decrease in flow regulation amplitude, with almost no significant change.

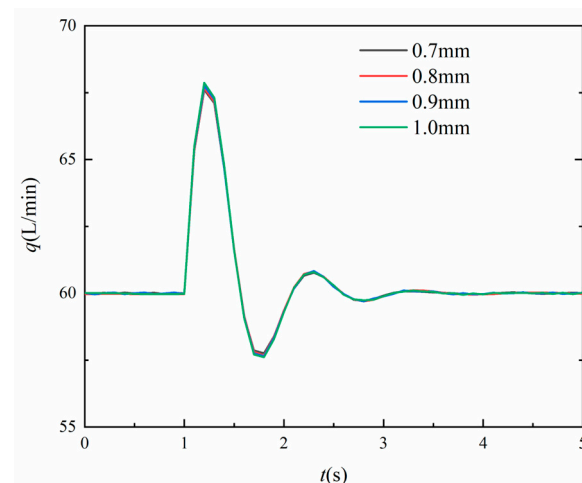


**Figure 7.** Flow curve under various diameters of damping hole 2.

### 3.1.3. The Influence of the Pilot Spring Stiffness on Flow Rate Variation

Figure 8 illustrates the impact of pilot spring stiffness on flow through the main spool. The simulation results indicate that the stiffness of the pilot spring significantly influences flow regulation. As the stiffness of the pilot spring increases, there is a noticeable decrease in both the amplitude of flow overshooting and oscillation.



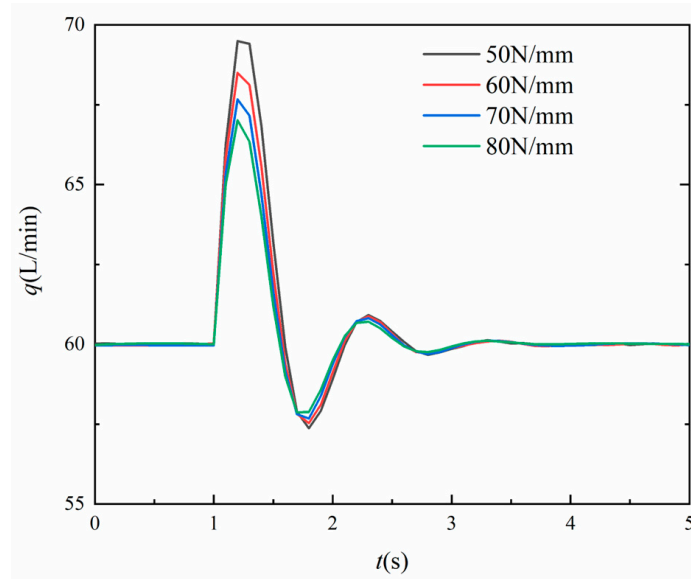


**Figure 8.** Flow curve under various diameters of pilot spring stiffness.

#### 3.1.4. The Influence of the Main Valve Spring Stiffness on Flow Rate Variation

Figure 9 illustrates the impact of the main spring stiffness on the flow rate through the main spool. The simulation results indicate that the influence of the main spring stiffness on flow regulation is minimal, and there is a slight decrease in the amplitude of flow overshoot with an increase in main spring stiffness.

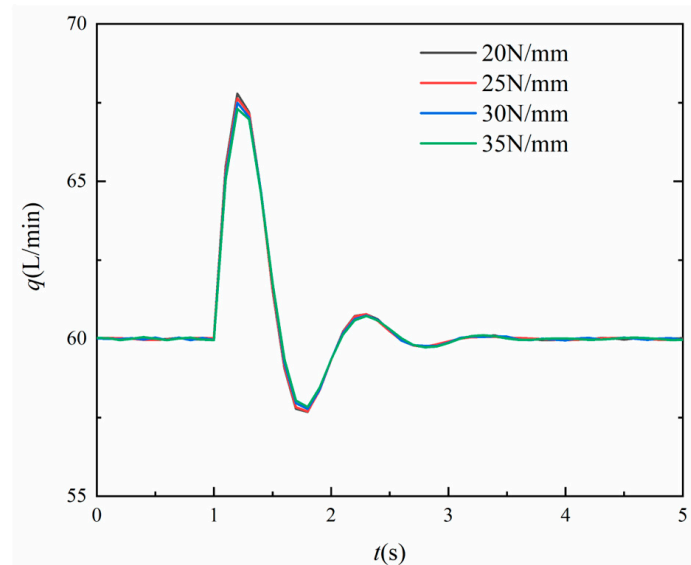


**Figure 9.** Flow curve under various diameters of main valve spring stiffness.

#### 3.1.5. The Influence of the Main Spool Seal Diameter on Flow Rate Variation

Figure 10 illustrates the impact of the main spool seal diameter on the flow through the main spool. The simulation results indicate that the main spool seal diameter has a significant influence on flow regulation. As the main spool seal diameter increases, there is a notable decrease in both flow overdrive and oscillation amplitude.

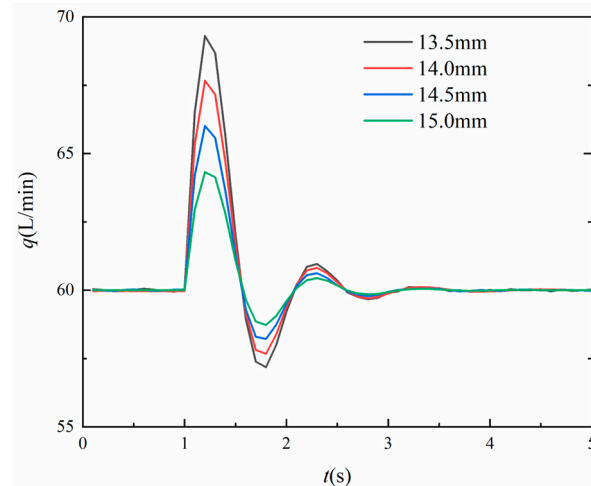


**Figure 10.** Flow curve under various diameters of main spool diameter.

### 3.1.6. The Influence of the Main Spool Upper Cavity Diameter on Flow Rate Variation

Figure 11 illustrates the impact of the diameter of the upper end of the main spool seal on the flow through the main spool. The simulation results indicate that the diameter of the upper end of the main spool significantly influences flow regulation, with a decrease in flow overshoot amplitude as the upper end diameter of the main spool increases.

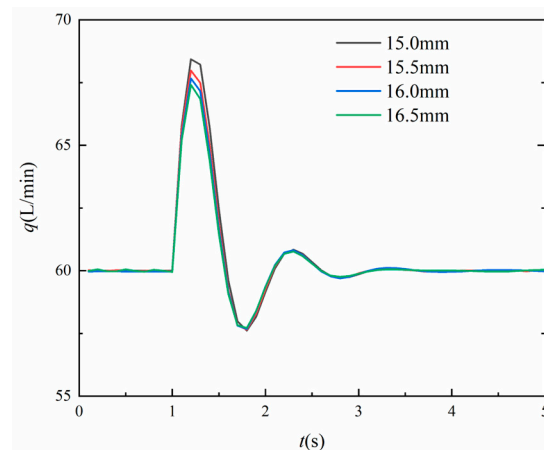


**Figure 11.** Flow curve under various diameters of main spool upper cavity diameter.

## 3.2. Structural Parameter Optimization Design

Based on the simulation analysis above, it is found that the diameter of damping holes 1 and 2 and the stiffness of the main spring have minimal impact on the flow through the main spool. On the other hand, the sealing diameter and upper end diameter of the main spool, as well as the stiffness of the pilot spring, have a significant influence. Therefore, it is essential to optimize these three parameters in order to enhance the dynamic response characteristics of flow regulation in the flow control valve.

### 3.2.1. Optimization Objectives

The primary goals of flow control are to minimize overshoot and oscillation. The ITAE (Integral Time Absolute Error) is a widely used performance evaluation index [18,19]. In this paper, the ITAE performance index is adopted as the evaluation criterion, and the objective function can be represented by the following formula:

$$\min J_{ITAE} = \int_0^{\infty} t|e(t)|dt \quad (5)$$

where  $e(t)$  is the difference between real-time traffic and target traffic at time  $t$ .

### 3.2.2. Optimal Results

The optimization of parameters for a new digital flow control valve presents a complex, multi-parameter, and nonlinear optimization problem. A genetic algorithm is a method used to search for the optimal solution by simulating the natural evolution process. It has been successfully employed in the parameter optimization of hydraulic system [20,21]. In this paper, AMESim is utilized to construct a simulation optimization model as depicted in Figure 12. The simulation model employs a genetic algorithm to optimize the parameters including the diameter of the main spool seal, the diameter of the upper end, and the stiffness of the pilot spring. The evaluation standard is based on ITAE index, with Formula (5) serving as the objective function.

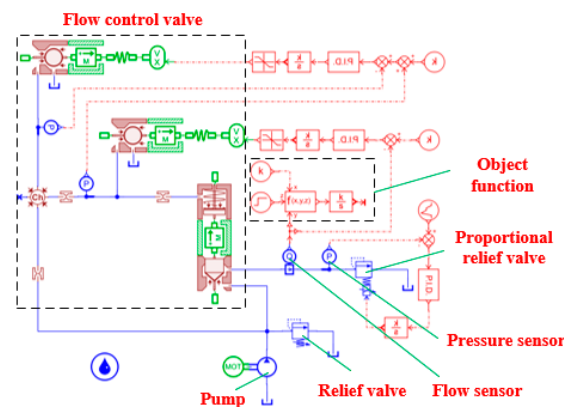


**Figure 12.** AMESim simulation optimization model based on genetic algorithm.

In the simulation model, the population size was set to 40, which was determined based on the number of parameters to be optimized combined with experience. The maximum number of iterations combined with computer performance and solution accuracy was set to 50, and the crossover rate and variation rate were set to 0.4 and 0.05, respectively, according to experience. Based on design experience of the hydraulic valve, initial values and upper/lower limits for three parameters are shown in Table 2. Other main parameters of the hydraulic system were set according to Table 1, while the parameters optimized by the genetic algorithm are also presented in Table 2. The flow curve before and after optimization is depicted in Figure 13.

**Table 2.** Upper and lower limits of parameters and parameters before and after optimization.

	Sealing Diameter of Main Valve Core/mm	Diameter of the Upper Chamber of the Main Valve Core/mm	Pilot Spring Stiffness/(N/mm)
Minimum value	13	15	60
Maximum value	15	17	90
Initial value	14	16	70
Optimal value	14.9	16.1	79.2

It is obvious from the comparison curve that the maximum overshoot percentage of flow regulation is reduced from 11.2% to 7%, which is an improvement of about 37.5%. The amplitude of oscillation was reduced from 9 L/min to 5.5 L/min, an improvement of about 45%. The frequency and response time of flow regulation oscillations are also somewhat decreased, and the optimized parameters exhibit improved dynamic response characteristics.

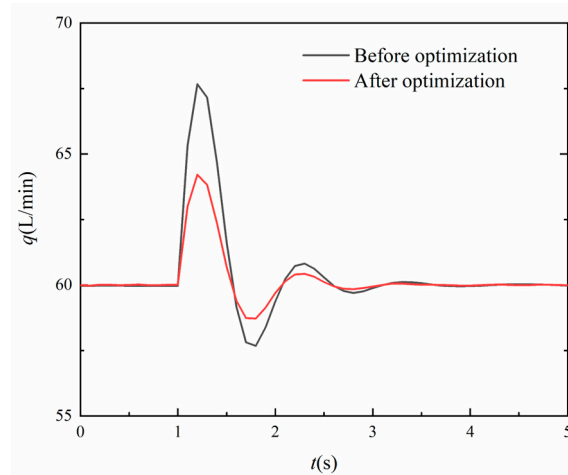


**Figure 13.** Response curve of flow characteristics before and after optimization.

## 4. Experimental Study

### 4.1. Experimental Device

In order to better verify the feasibility and progressiveness of the developed flow control valve, a test system was built as shown in Figure 14. The experimental system consists of an emulsion pump, digital sequence valve, proportional relief valve, emulsion motor, servo motor, rectifier device, pressure sensor, flow sensor, computer, controller, etc. The emulsion discharged by the emulsion pump enters the digital sequence valve and the proportional relief valve respectively. The inlet pressure of the digital sequence valve can be adjusted by controlling the proportional relief valve, and the outlet pressure of the digital sequence valve can be adjusted by controlling the servo motor. When the pressure difference between the inlet and outlet changes, flow regulation can be achieved by adjusting the linear stepper motor of the digital sequence valve. The emulsion pump in this system is a fixed displacement pump with a nominal flow rate of 125 L/min.

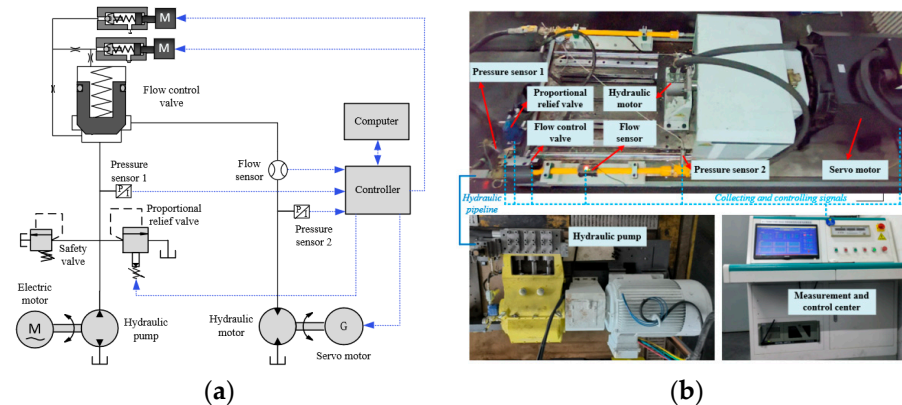


**Figure 14.** Experimental platform. (a) Experimental system schematic diagram; (b) physical diagram of the experimental system.

### 4.2. Experimental Study on Stability of Flow Regulation

A new prototype flow control valve was developed, and its three-dimensional model and physical model are depicted in Figure 15. To validate the flow regulation stability of the flow control valve, a comparison was made with a flow control valve featuring a single pilot spool. The three-dimensional model and physical model of this comparison valve are shown in Figure 16.

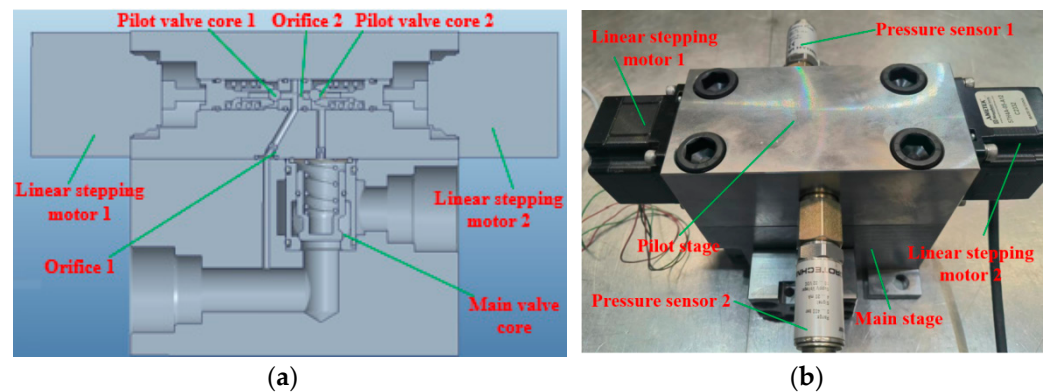


**Figure 15.** 3D model and prototype of a digital flow control valve with a dual pilot valve core structure. (a) 3D model; (b) prototype model.

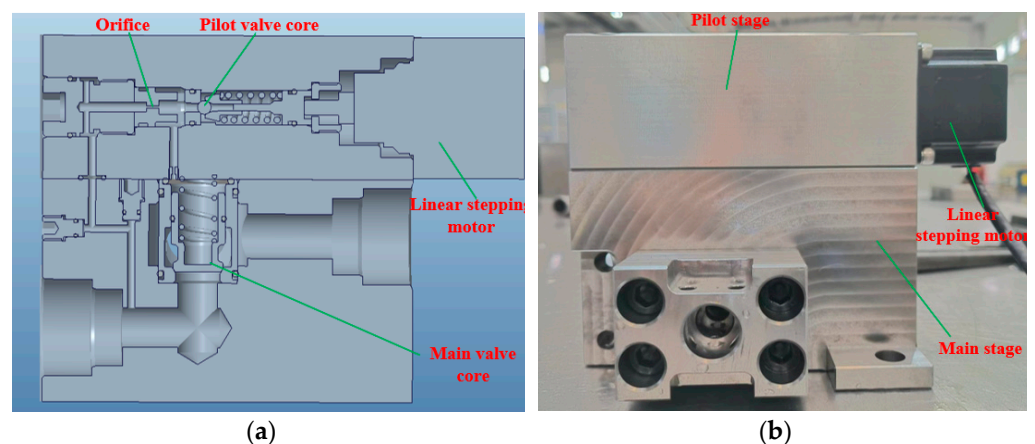


**Figure 16.** 3D model and prototype of a digital flow control valve with a single pilot valve core structure. (a) 3D model; (b) prototype model.

The experimental setup depicted in Figure 12 was utilized to conduct experiments on two different structures of flow control valves. The testing method was as follows: Firstly, the single-pilot flow control valve was selected as the specimen for testing. The extension of the linear stepping motor shaft of the pilot stage was adjusted to 1.65 mm, and the proportional relief valve was adjusted to maintain the inlet pressure of the main spool at 80 bar. Additionally, the hydraulic motor servo motor was adjusted to keep the outlet pressure of the main spool at 15 bar. The flow curve through the main spool was then recorded, as depicted in Figure 17. Subsequently, the double pilot flow control valve was replaced as the test piece. The axial extension of the linear stepping motor of pilot stage 1 was adjusted to 1 mm. Based on the feedback from the pressure sensor in front of the pilot valve spool, the linear stepping motor of pilot stage 2 was adjusted to maintain a constant pressure difference before and after damping hole 2 at 10 bar. Similarly, the inlet and outlet pressures of the main spool were set to 80 bar and 40 bar, respectively. The flow curve through the main spool was recorded as shown in Figure 17. The experimental results indicate that the spool structure with a double pilot stage exhibits a more stable flow curve and better flow regulation stability compared to that with a single pilot stage.

From the experimental curve, it can be seen that the new structure sequence valve has more obvious pressure flow characteristics compared to the traditional structure sequence valve, which is consistent with the simulation results. However, under the same compression amount and flow rate of the pilot spring, the experimental data have a higher pressure difference than the simulation data, which is due to the additional flow resistance generated in pipelines, joints, and other areas.

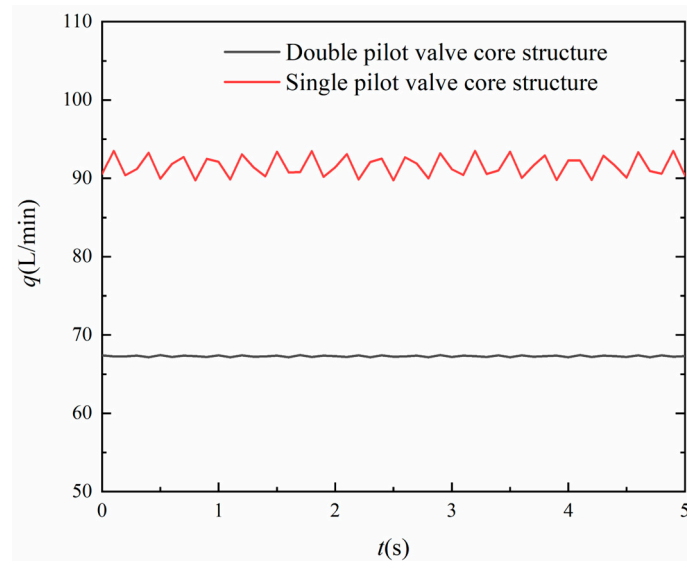


**Figure 17.** Flow curves of two types of flow control valves.

#### 4.3. Experimental Study of Flow Regulation Characteristics

The test platform depicted in Figure 12 was utilized for testing both the double pilot stage flow control valve and the single pilot stage flow control valve. The specific testing methods were as follows: The target value of flow through the main spool was consistently set at 60 L/min, while the target value of inlet pressure of the main spool of the flow control valve was always set at 70 bar, and the target value of outlet pressure suddenly increased from 15 bar to 20 bar. The change in flow through the main spool during the process of pressure change was monitored, and a response curve of flow regulation was drawn, as shown in Figure 18.

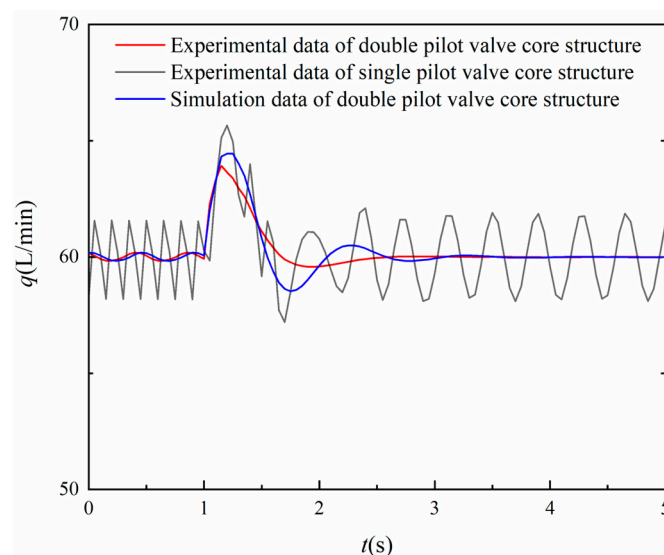


**Figure 18.** Flow characteristic response curve.

Based on the test results, it is evident that the flow curve of the optimized dual pilot spool structure aligns closely with the simulation data. However, there was a reduction in oscillation amplitude to some extent. This can be attributed to the fact that during actual testing, the flow sensor records an average value over a certain period of time, and also operates at a relatively low sampling frequency. It also can be observed from the curve that the double pilot spool structure exhibits smaller flow regulation deviation and higher adjustment stability compared to the single pilot spool structure. This demonstrates that



the double pilot spool structure possesses superior dynamic influence characteristics and a more effective flow regulation effect.

## 5. Summary

This paper introduces a novel digital flow control valve for high-pressure water hydraulic systems. The valve utilizes a double pilot valve core structure and a linear stepping motor as the driving device. In this paper, the mathematical model and AMESim simulation model of the flow control valve are established. It is analyzed that the new structure of the flow control valve can achieve flow regulation in both high- and low-pressure water hydraulic systems, with high stability in flow regulation. Secondly, the study investigates the influence of structural parameters on the dynamic characteristics of flow regulation. It is emphasized that the stiffness of the pilot spring, the sealing area of the main spool, and the diameter of the upper end of the main spool significantly impact the dynamic response characteristics of flow regulation. A genetic algorithm based on ITAE performance index was employed to optimize these three parameters. The simulation results indicate that the optimized flow control valve reduces the maximum overshoot amplitude of flow regulation by approximately 45%. This suggests a significant improvement in the performance of the valve. Finally, this paper presents the development of two types of prototypes for digital flow control valves: single pilot stage and double pilot stage. Additionally, a test platform was established for conducting tests on these prototypes. The test results were found to be in line with the simulation results, thus confirming the performance advantages of the new structure digital flow control valve and the accuracy of parameter optimization design.

**Author Contributions:** Conceptualization, J.T. and W.L.; methodology, W.L.; software, H.W. and J.L.; validation, J.L. and R.Z.; formal analysis, W.L. and R.Z.; investigation, W.L.; resources, J.T.; data curation, W.L. and Y.C.; writing—original draft preparation, W.L. and H.W.; writing—review and editing, W.L. and J.T.; visualization, Y.C.; supervision, R.Z.; project administration, J.L.; funding acquisition, J.T. All authors have read and agreed to the published version of the manuscript.

**Funding:** The authors appreciate for the fiscal encourage from the Fundamental Research Funds for the Central Universities under Grant (2022JCCXJD02 and 2022YJSJD09), the Ministry of Education (EW202180222), and the National Natural Science Foundation of China under Grant (51774293).

**Data Availability Statement:** The original contributions presented in the study are included in the article, further inquiries can be directed to the corresponding author.

**Conflicts of Interest:** Authors Junshi Li and Rulin Zhou were employed by the company Beijing Tianma Intelligent Control Technology Co., Ltd. The remaining authors declare that the research was conducted in the absence of any commercial or financial relationships that could be construed as a potential conflict of interest.

## References

1. Wang, Z.; Liu, Y.; Cheng, Q.; Pang, H.; Ma, Y.; Zhao, S.; Wang, W.; Wu, D. Dynamic characteristics evaluation of balance valve for seawater hydraulic variable ballast system considering the depth variation. *Ships Offshore Struct.* **2022**, *19*, 252–262. [[CrossRef](#)]
2. Zhou, R.; Meng, L.; Yuan, X.; Qiao, Z. Research and Experimental Analysis of Hydraulic Cylinder Position Control Mechanism Based on Pressure Detection. *Machines* **2022**, *10*, 1. [[CrossRef](#)]
3. Rodríguez-Pérez, Á.M.; Rodríguez, C.A.; Márquez-Rodríguez, A.; Mancera, J.J.C. Viability Analysis of Tidal Turbine Installation Using Fuzzy Logic: Case Study and Design Considerations. *Axioms* **2023**, *12*, 778. [[CrossRef](#)]
4. Tian, J.; Liu, W.; Wang, H.; Yuan, X.; Zhou, R.; Li, J. Energy-Saving Testing System for a Coal Mine Emulsion Pump Using the Pressure Differential Flow Characteristics of Digital Relief Valves. *Processes* **2023**, *11*, 2632. [[CrossRef](#)]
5. Han, M.; Liu, Y.; Wu, D.; Zhao, X.; Tan, H. A numerical investigation in characteristics of flow force under cavitation state inside the water hydraulic poppet valves. *Int. J. Heat Mass Transf.* **2017**, *111*, 1–16. [[CrossRef](#)]
6. Li, J.; Zhang, Q.; Zhang, Y.; Peng, C.; Yang, Y. Modeling and Simulation Analysis of Speed-Regulating Valve Flow Fluctuations under Differential Pressure Steps. *Electronics* **2022**, *11*, 2580. [[CrossRef](#)]
7. Tang, Y.; Zhou, M.; Liu, X.; Li, G.; Wang, Q.; Wang, G. Study on throttling pressure control flow field for traction speed regulation and braking mechanism of the pipeline intelligent plugging robot. *Energy* **2023**, *282*, 128331. [[CrossRef](#)]

8. Kushwaha, P.; Dasgupta, K.; Ghoshal, S. A comparative analysis of the pump controlled, valve controlled and prime mover controlled hydromotor drive to attain constant speed for varying load. *ISA Trans.* **2022**, *120*, 305–317. [[CrossRef](#)]
9. Lin, Y.; Lin, T.; Li, Z.; Ren, H.; Chen, Q.; Chen, J. Throttling Loss Energy-Regeneration System Based on Pressure Difference Pump Control for Electric Forklifts. *Processes* **2023**, *11*, 2459. [[CrossRef](#)]
10. Xu, C.; Ren, Y.; Tang, H.; Lu, L.; Huang, Y.; Ruan, J. Investigation on a novel high frequency two-dimensional (2D) rotary valve variable mechanism for fluid pulse-width-modulation application. *Mech. Sci. Technol.* **2023**, *37*, 757–765. [[CrossRef](#)]
11. Xie, S.; Song, Z.; Huang, J.; Zhao, J.; Ruan, J. Characterization of two-dimensional cartridge type bidirectional proportional throttle valve. *Flow Meas. Instrum.* **2023**, *93*, 102434. [[CrossRef](#)]
12. Zhang, H.; Liao, Y.; Tao, Z.; Lian, Z.; Zhao, R. Modeling and Dynamic Characteristics of a Novel High-Pressure and Large-Flow Water Hydraulic Proportional Valve. *Machines* **2022**, *10*, 37. [[CrossRef](#)]
13. Wang, H.; Wang, X.; Huang, J.; Quan, L. Flow Control for a Two-Stage Proportional Valve with Hydraulic Position Feedback. *Chin. J. Mech. Eng.* **2020**, *33*, 93. [[CrossRef](#)]
14. Han, M.; Liu, Y.; Zheng, K.; Ding, Y.; Wu, D. Investigation on the modeling and dynamic characteristics of a fast-response and large-flow water hydraulic proportional cartridge valve. *Proc. Inst. Mech. Eng. Part C J. Mech. Eng. Sci.* **2020**, *234*, 4415–4432. [[CrossRef](#)]
15. Tian, J.; Liu, W.; Wang, H. Testing Method for Intelligent Loading of Mining Emulsion Pump Based on Digital Relief Valve and BP Neural Network Control Algorithm. *Machines* **2022**, *10*, 896. [[CrossRef](#)]
16. Park, S. Development of a proportional poppet-type water hydraulic valve. *Proc. Inst. Mech. Eng. Part C J. Mech. Eng. Sci.* **2009**, *223*, 2099–2107. [[CrossRef](#)]
17. Park, S.; Kitagawa, A.; Kawashima, M. Water hydraulic high-speed solenoid valve Part 1: Development and static behaviour. *Proc. Inst. Mech. Eng. Part I J. Syst. Control. Eng.* **2004**, *218*, 399–409. [[CrossRef](#)]
18. Chen, P.; Luo, Y.; Peng, Y.; Chen, Y. Optimal Fractional-Order Active Disturbance Rejection Controller Design for PMSM Speed Servo System. *Entropy* **2021**, *23*, 262. [[CrossRef](#)]
19. El-Sehiemy, R.; Shaheen, A.; Ginidi, A.; Al-Gahtani, S. Proportional-Integral-Derivative Controller Based-Artificial Rabbits Algorithm for Load Frequency Control in Multi-Area Power Systems. *Fractal Fract.* **2023**, *7*, 97. [[CrossRef](#)]
20. Sharafati, A.; Tafarjnoruz, A.; Shourian, M.; Yaseen, Z. Simulation of the depth scouring downstream sluice gate: The validation of newly developed data-intelligent models. *J. Hydro-Environ. Res.* **2020**, *29*, 20–30. [[CrossRef](#)]
21. Rodríguez-Pérez, A.; Rodríguez, G.C.; López, R.; Hernández-Torres, J.; Caparrós-Mancera, J. Water Microturbines for Sustainable Applications: Optimization Analysis and Experimental Validation. *Water Resour. Manag.* **2024**, *38*, 1011–1025. [[CrossRef](#)]

**Disclaimer/Publisher’s Note:** The statements, opinions and data contained in all publications are solely those of the individual author(s) and contributor(s) and not of MDPI and/or the editor(s). MDPI and/or the editor(s) disclaim responsibility for any injury to people or property resulting from any ideas, methods, instructions or products referred to in the content.